ELSEVIER

Tectonophysics 290 (1998) 27–45

TECTONOPHYSICS

Viscoelastic behavior of partially molten granites

Nikolai Bagdassarov [a,*], Alexander Dorfman [b,1]

[a] *Institut für Meteorologie und Geophysik, J.W. Goethe Universität Frankfurt, Feldbergstraße 47, D-60323 Frankfurt/Main, Germany*
[b] *Bayerisches Geoinstitut, Universität Bayreuth, D-95440 Bayreuth, Germany*

Received 12 May 1997; accepted 21 November 1997

Abstract

Effects of partial melting on complex shear modulus (G^*) and internal friction (Q^{-1}) of granites have been investigated using a torsion-deformation apparatus in the frequency range of 2 mHz–20 Hz at 650–1250ºC. Granite samples from Kirchberg/W. Erzgebirge, Germany (OG1) and fine-grained quartz-feldspar porphyry Åland/SW Finland (QFP) have been annealed for ≈30 h at temperatures of 1175ºC and 1150ºC, 1 bar, $\log[f_{O_2}] \approx -11.7$. The partially molten OG1 samples contained $\approx 40 \pm 2$ vol% solid phase, QFP samples ≈55–60 vol%, mainly of quartz crystals. Two different viscoelastic behaviors have been observed: melt-dominated viscoelasticity below a critical quartz-crystal concentration (≈40 vol%) for OG1 samples and weak elastic behavior caused by mechanical interaction between crystals above a critical crystal concentration (≈55–60 vol%) in QFP samples. For OG1 samples the Newtonian relaxed viscosity is observable at high-temperature–low-frequency conditions. For QFP samples the Newtonian relaxed viscosity is unattainable, either by torsion deformation (strain rate up to 10^{-2} s^{-1}) or by dilatometry (strain rate up to 10^{-5} s^{-1}). The internal friction $\log[Q^{-1}(\omega\tau)]$ (where ω is angular frequency, τ is shear-stress relaxation time) for partially molten samples plotted on a double-log plot vs. normalized frequency $\omega\tau$ has different slopes above and below $\omega\tau = 1$. For OG1 and QFP samples at $\omega\tau \gg 1$ the slope of $\log[Q^{-1}(\omega\tau)]$ is ~ -0.5 to -0.55 and does not depend on the volume fraction of crystals. In OG1 sample at $\omega\tau \ll 1$ this slope is -0.45. In QFP samples the slope is ≈0 and the internal friction is practically independent of $\omega\tau$ at the high temperature–low frequency limit $Q^{-1}(\omega\tau \Rightarrow 0) \approx 2$. In sample OG1 where the crystal content lies below the rheological critical concentration, the observed dependencies of $G(\omega\tau)$ and $Q^{-1}(\omega\tau)$ are related to a power-law Q-body with the exponent ∼0.5. In sample QFP where crystal contents are above the rheological critical value, the mechanical contacts between crystals determine a weak elastic behavior of the suspension ascribed to a Caputo-body stress relaxation function with the exponent ∼0.55. The imaginary component of the shear modulus $G'(\omega\tau)$ for sample OG1 is asymmetrical with an extended shoulder $\omega\tau \gg 1$. In sample QFP $G''(\omega\tau)$ has a symmetrical shape. The difference between effective shear viscosity of partially molten granite with 40 vol% of crystals and shear viscosity of the partial melt may be of 3 log(Pa s) units. Thus, the effective shear viscosity of partially molten granite (40–50 vol% of crystals) is close to the shear viscosity of the melt phase having the same bulk composition. A model of temperature and frequency dependencies of the complex shear-wave velocity based on the experimentally determined parameters has been suggested for partially molten granites.

Keywords: partial melting; granites; rheology; viscoelastic behavior; complex shear modulus; internal friction

* Corresponding author. Fax: +49 69 79823280; E-mail: nickbagd@geophysik.uni-frankfurt.de
[1] Present address: Vernadsky Institute of Geochemistry, Russian Academy of Sciences, Kosygin str. 19, 117975 Moscow, Russia.

0040-1951/98/$19.00
PII S0040-1951(98)00010-9

1. Introduction

Lithospheric rocks containing a fraction of silicate liquid as a result of partial melting represent a special group of anelastic geomaterials. Locations of rocks with partial melt in the crust and in the upper mantle are of particular interest to geoscientists. Partially melted zones in the lithosphere have been established from field data on the attenuation of seismic waves, from geoelectric data and from gravity anomalies. Interpretation of the seismic data is strongly dependent on how well we know high-temperature anelastic behavior and attenuation in rocks (Berckhemer et al., 1982; Jackson and Paterson, 1987). This explains why high-temperature measurements of elastic moduli of rocks and minerals, internal friction and their frequency dependencies are the subject of many laboratory experiments (e.g. Jackson, 1986; Jackson et al., 1992).

Partially molten rocks may show a transient creep with transient elastic moduli and transient viscosities (Smith and Carpenter, 1987). The transient rheology of rocks is mainly due to the strain-dependent frictional resistance resulting from grain surface processes like local dilatation of grain boundaries, degradation of surface roughness, and reshaping of the sliding grains (Leong and Randolph, 1992). The widely accepted view that all lithospheric rocks flow according to a power-law creep model may be reconsidered in future, and under certain P–T conditions other rheologies may dominate (Tsenn and Carter, 1987). At low stresses the flow regime of polycrystalline rocks more likely corresponds to a diffusional creep, at intermediate stresses to a power law creep ($\dot{\epsilon} = \text{const}\cdot\sigma^n$), and at high stresses to an exponential creep ($\dot{\epsilon} = \text{const}\cdot\exp(\beta\sigma)$). By low stresses here we understand the range of differential stresses in which there are no stress effects on the transport properties of diffusing species, i.e. differential stresses contribute linearly to the gradient of chemical potential of diffusing species. Thus, partially molten rocks, depending on the degree of partial melting and level of stresses, may also behave as Newtonian liquids or obey the power law or exponential creep law, depending on the relative amplitude of stresses to the stiffness of the rock.

Experimental and theoretical studies of rheology and mechanisms of anelasticity of partially molten rocks in the Earth may significantly improve our understanding of their rheology. In recent years in some petrophysical laboratories special attention has been drawn to viscoelastic and creep models of two-phase and polyphase aggregates consisting of components with contrasting strength and creep parameters. Nevertheless, to the best of our knowledge until now few experiments have been performed on the viscoelastic properties of partially molten rocks at high degrees of partial melting.

A model of rheology or a flow law which is applicable to partially molten lithospheric rocks may be constrained from the direct dynamic measurements of the complex shear modulus (G^*) and the internal friction (Q^{-1}) on lithospheric rocks at seismic frequencies and high temperatures. This work deals with the measurement of a complex shear modulus and internal friction in partially molten granites with about 40 and 60 vol% of melt at small shear stresses using seismic frequencies and in the temperature range of liquid-phase softening.

2. Sample description and preparation

The granite samples chosen for the experiments were a biotite–monzogranite from the Kirchberg massif, West Erzgebirge, Germany (OG1) and a fine-grained quartz-feldspar porphyry from Åland, southwest Finland (QFP). Their chemical compositions are given in Table 1 (Tischendorf et al., 1987; Lindberg and Eklund, 1992). Samples were chosen because of the small size of crystals (<1 mm), mechanical homogeneity and the absence of cracks and alterations (Fig. 1).

The aplite sample OG1 is the youngest phase of granites in the Kirchberger massif (Gerstenberger et al., 1995). The modal composition of sample OG1 is: plagioclase ($An_{30–20}$) 36.3 vol%, quartz 27%, perthitic orthoclase 10.5%, trioctahedral mica (presented as Fe- and Mg-biotite) 8.1%, microcline 16.8% (Tischendorf, 1989).

The fine-grained quartz-feldspar porphyry sample QFP consists of some xenocrysts of K-feldspar, quartz with an average size of 300–500 μm, plagioclase (An_{33}). The location of QFP is on the southwestern contact between the Åland rapakivi batholith and the Svecofennian country rocks. The rock is believed to be a product of a bimodal igneous event

Table 1
Chemical composition of the granites studied

Oxide (wt.%)	QFP (bulk)	QFP (melt) ± st.err	OG1 (bulk)	OG1 (melt) ± st.err
SiO_2	76.20	65.39 ± 0.54	76.90	65.88 ± 1.28
TiO_2	0.22	0.10 ± 0.08	0.055	0.05 ± 0.03
Al_2O_3	11.50	18.59 ± 0.24	13.00	19.58 ± 0.83
FeO	2.17	0.77 ± 0.30	0.63	0.23 ± 0.27
MnO	0.12	0.06 ± 0.06	0.02	0.03 ± 0.03
MgO	0.43	0.29 ± 0.20	0.02	0.08 ± 0.07
CaO	2.63	0.84 ± 0.28	0.36	0.76 ± 0.23
Na_2O	2.31	3.64 ± 0.07	3.59	5.65 ± 0.69
K_2O	5.64	10.32 ± 0.23	5.38	7.73 ± 0.88
F	0.026		0.02	
P_2O_5	0.04	0.01 ± 0.01	0.016	0.02 ± 0.02
Rb	190 ppm		523 ppm	
Zr	260 ppm		90 ppm	
Sum	101.29	100.01	99.99	100.01

Bulk = initial bulk chemical composition (determined from wet chemistry analysis); melt = chemical analysis of partial melt (average of 10 analysis determined from a Camebax SX50 microprobe, at 15 kV, 15 nA, beam spot 2 μm).
[a]OG1 = aplite sample from the Kirchberger massif/westerzgebirge, Germany (Tischendorf et al., 1987). Rock age: 309 ± 4 Ma (Sr geochronology).
[b]QFP = fine-grained quartz-feldspar porphyry from Åland rapakivi batholith, subvolcanic Hammarudda complex, SW Finland (Lindberg and Eklund, 1992). Rock age: 1571 ± 9 Ma (U/Pb geochronology).

and it carries mafic enclaves (Lindberg and Eklund, 1992). The mafic enclaves in the granite sample have a spongy morphology composed of a cellular mantle of Na-rich plagioclase and a Ca-rich core which is a result of the cellular plagioclase intergrowth (Andersson and Eklund, 1994). Patchy zones have a length of 0.5 mm and the length of intergrowth cells may be as small as 20 μm. The mafic enclaves were formed by magma mixing and mingling when monzodioritic and granitic magmas flowed through a dike (Andersson and Eklund, 1994). This spongy character of crystals in the starting sample determines the microgeometry of partial melting.

Rectangular bars (10 cm × 2 cm × 2 cm) from cobbles of granitic rocks of OG1 and QFP were placed in a furnace with controlled oxygen fugacity $\log[f_{O_2}] = -11$ for 24–30 h at temperatures of 1175 and 1150ºC, respectively. Oxygen fugacity was controlled by using a CO/CO_2 gas mixture. The bars were cooled down slowly to room temperature over 24 h in order to suppress thermal cracking. Cylinders (diameter 8 mm, length 35 mm) were cored from the prepared bars.

Microgeometry and 2-D volume fraction of melt before and after deformation experiments were estimated from the image analysis of thin and polished sections of samples using an optical microscope and SEM combined with a Tracor Nothern TN-8500® Image Analysis System. The chemical composition of partial melts was obtained using the Cameca microprobe Camebax SX50 and results are listed in Table 1. A certain degree of partial melting was achieved during the preparation of the sample over a time much longer than the duration of measurements in the torsion device. Optical inspection and analysis of thin sections of samples after torsion-deformation experiments did not show changes of the degree of partial melting by >1–2 vol%.

The prepared granite samples contained partial melt and crystalline grains, mostly of quartz. They did not contain water, which had been lost during preparation of the samples. In sample OG1, the volume fraction of the quartz crystals was 40 ± 2 vol%. Melt forms a matrix, and quartz-crystals with a size <0.5 mm (dark-gray color in Fig. 1a and b) were suspended in the melt (light-gray color). The partially molten sample QFP contains 55–60 vol% of quartz crystals. In the sample of QFP quartz and Ca-rich plagioclase (An_{50}) crystals form a spongy texture surrounded by melt (dark- and light-grey in Fig. 1c

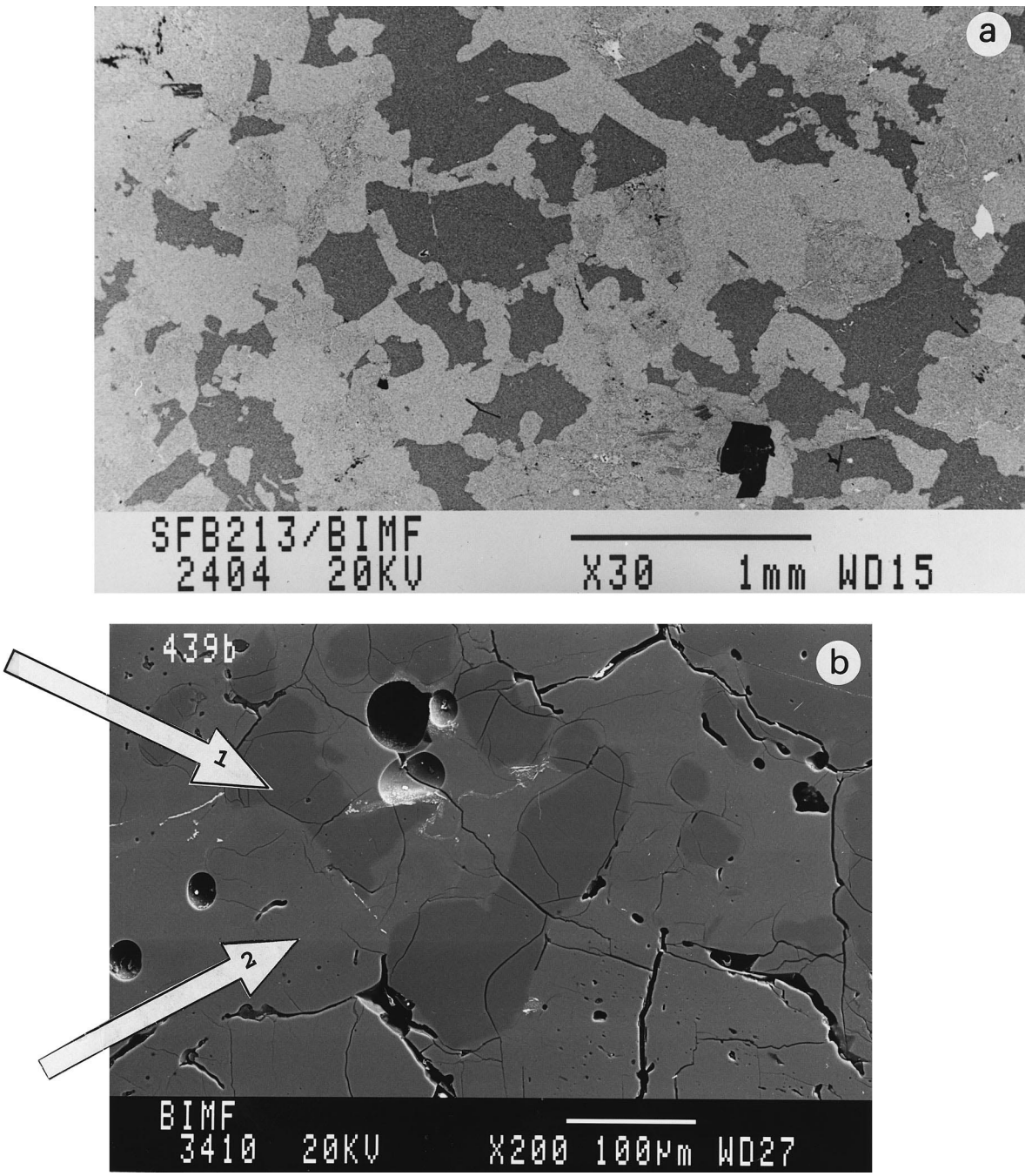

Fig. 1. Scanning electron microscopy of partially molten granite samples annealed in a furnace with controlled oxygen fugacity $\log[f_{O_2}] = -11.7$. (a, b) Aplite Kirchberg (OG1) annealed at 1175ºC for 24 h, crystal content 40 ± 2 vol%; *1* = quartz crystals, *2* = partial melt.

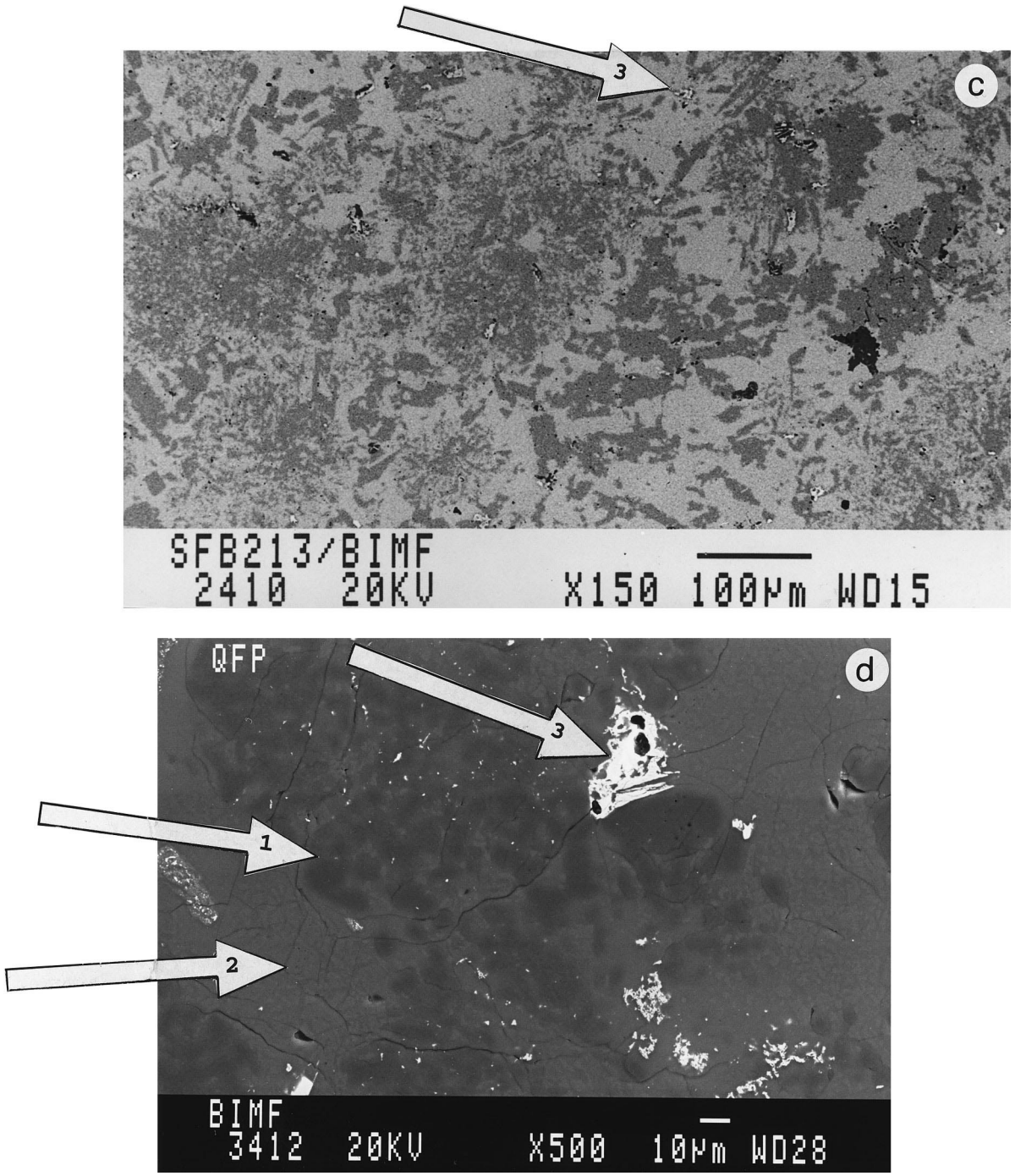

Fig. 1 (continued). (c, d) Fine-grained quartz feldspar porphyry of Åland (QFP) annealed at 1150ºC for 30 h, crystal content 55–60 vol%; *1* = plagioclase crystals forming a spongy texture, *2* = partial melt, *3* = Ti–Mt-crystal.

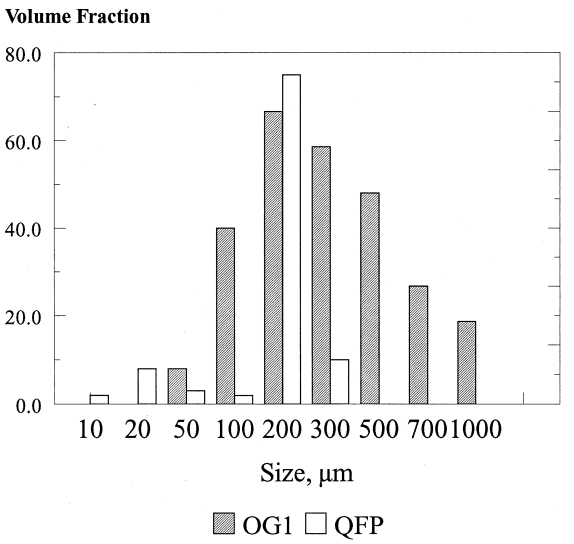

Fig. 2. 2-D size distribution of crystals (vol%) in partially molten granite samples obtained from the image analysis of thin sections.

and d indicate crystals and melt, respectively). Small amounts of Fe–Ti oxides (white colour) were also present in partially molten samples (white colour in Fig. 1d). The volume fraction of titanomagnetite crystals with an average size <5 μm in sample OG1 is <1 vol%. In the QFP sample there are 1–2 vol% of titanomagnetite grains with sizes between 5–20 μm. The 2-D size distribution statistics of crystals in the partially molten granite samples are shown in Fig. 2. The melt–crystal suspension of QFP samples has two characteristic crystal sizes. A cluster size of the variolitic type of texture is 100–200 μm, and the cluster size within the cellular zones is 20 μm. This complex character of partial-melt microgeometry mimics the microgeometry of mafic enclaves with spongy morphology in the starting QFP samples.

3. Experimental procedure

The viscoelastic behavior of partially molten granite samples was characterized by complex shear modulus and internal friction measurements in the temperature range 700–1230ºC and in the frequency range 20–0.002 Hz using an oscillatory torsion-deformation device (Berckhemer et al., 1982; Bagdassarov and Dingwell, 1993). The essential elements of the torsion-deformation apparatus are shown in Fig. 3. The method of shear modulus measurements is based on the small angle deformation of cylindrical samples under known torque applied at a certain frequency (Kampfmann, 1984). The apparatus consists of a high-temperature horizontal furnace, an assembly of two alumina rods (diameter 8 mm, length 190 mm, AL23, Frialit®–Degussite™) placed inside the furnace, and an electromagnetic coil system providing forced harmonic oscillations. The oscillatory torque is applied to the mechanical system consisting of two alumina rods and the sample mounted tightly between them. Slip between alumina rods and the sample has been eliminated using a special frictional junction between the rods with the sample and a high temperature cement, Polytec®. The duration of the complex shear modulus measurements at any temperature in the frequency range 20–0.002 Hz is about 35 min. At temperatures above 1120ºC the low-frequency measurements (0.002–0.05 Hz) were excluded and the total duration of measurements did not exceed 8–12 min.

In the experiments on partially molten granites the flat ends of cylindrical samples were machined to conical shapes (see inset in Fig. 3). Similar inverted conical holes (4 mm in max. diameter, 5 mm in length) were machined on the flat ends of alumina rods. By applying a small axial load to the system of two alumina rods and the sample during experiments the friction between conical surfaces of rods and the sample provides a good mechanical contact that has been checked in a test with a sample of alumina ceramic AL23 (Frialit®–Degussite®). Mechanical deformation of the system (two rods + sample) is registered at two points using two pairs of capacitive pick-ups. Conversion of electrical signals (μV) into mechanical displacement (μm) and mechanical torque were done using a special calibration of the mechanical system made by applying a known static torque (10^{-5} to 10^{-4} N m) or rotating the system to a known angle (10^{-4} to 10^{-3} rad). The calibration and data processing of electrical signals are described elsewhere (Bagdassarov and Dingwell, 1993). Data processing of stored signals permitted a characterization of the shear modulus (with an absolute precision of 5%) and the phase angle between applied torque and resulting strain (with a precision of 5×10^{-4} rad) for the tested cylindrical sample at a given temperature and frequency.

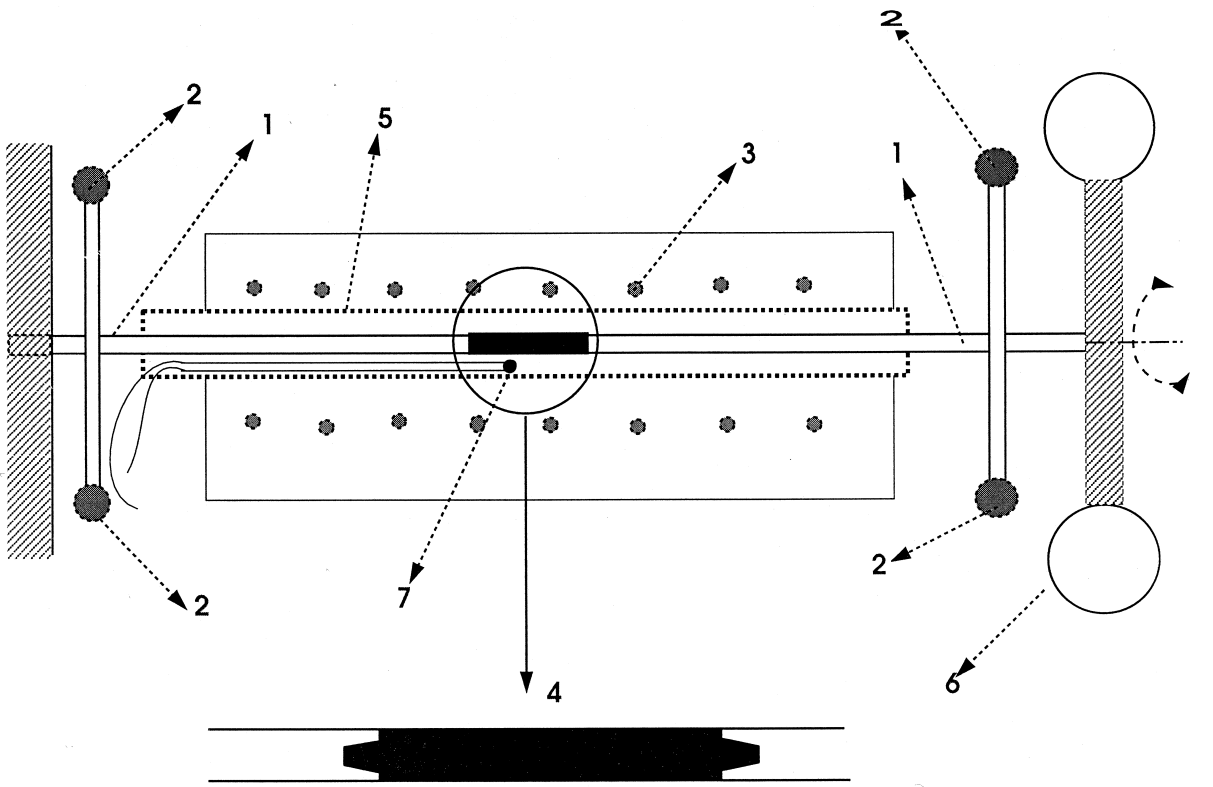

Fig. 3. Principles of the operation of the oscillatory torsion deformation device. A sample is fixed between two alumina rods. The sample (*4*) is set between two alumina rods in the tube furnace (*3*). The end of the right ceramic alumina rod (*1*) is fixed. To the left alumina rod via the coil electromagnets (*6*) the sinusoidal oscillation is applied. Conical grips on the sample and inverted conical holes in the alumina rods prevent the slip in the mechanical system under torsion. (*2*) are capacity pick-ups, (*5*) is alumina tube, (*7*) is thermocouple.

Compressional viscosity of partially molten granite samples was measured using a BÄHR DIL 802 V vertical push rod dilatometer with the alumina holder in an Ar gas flow using parallel-plate viscometry. The method of viscosity measurement, the calibration procedure and the principle of data processing are described elsewhere (Bagdassarov and Dingwell, 1992). Variation of stress between 1.9×10^4 and 7.6×10^4 Pa was achieved using cylindrical samples (10–12 mm in length) with different diameters (5–10 mm) under a vertical force of 1.5 N. The compression of the sample has been monitored at a fixed temperature after loading and unloading with a time step of 15 s over 2–6 h depending on the strain rate. During the first 30–40 min after the application of the compressive stress the rheological behavior of the partially molten sample was not perfectly steady-state, and this time interval was excluded from the calculation of shear viscosity. The cumulative longitudinal strain in each experiment did not exceed 5%. Accuracy of shear viscosity measurements using this method was checked against a reference material (lead-silica glass NBS 711) at a temperature of 487ºC, and the tabulated value was reproduced within ± 0.06 $\log_{10}$ Pa s or better than 1% at viscosity 10^9 Pa s.

4. Shear viscosity

The maximum amplitude of strain at the outer interface of the cylindrical specimens in torsion experiments was 10^{-5}. The small torsional deformation of a cylindrical sample with a diameter much smaller than the length provides a simple shear and linear type of deformation. In this case the angle through which the sample is deformed, is linearly proportional to the applied torque (e.g. Bagdassarov and Dingwell, 1993). The oscillatory shear mea-

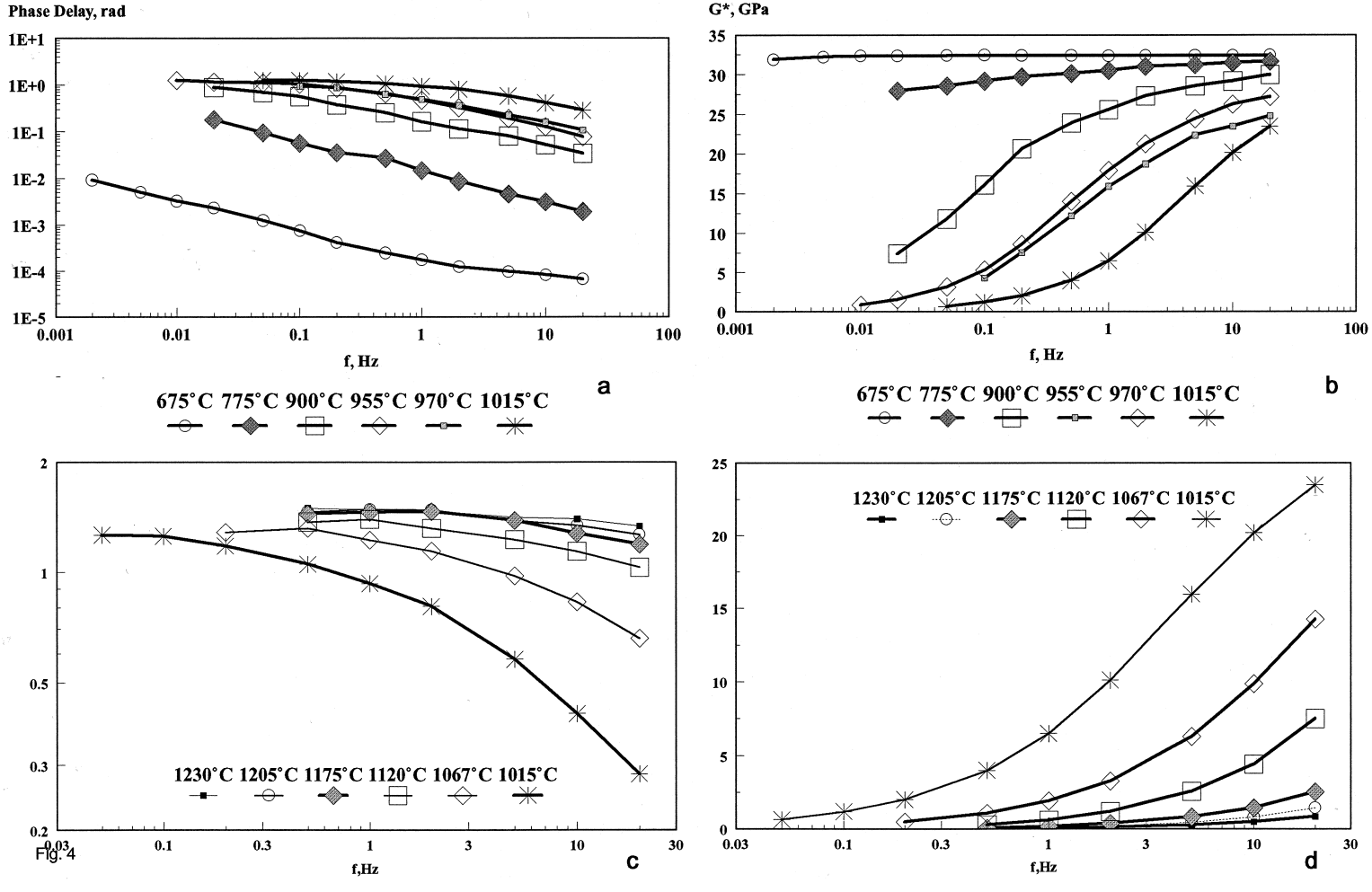

Fig. 4

Fig. 4. Phase shift φ (a) and (c) and shear modulus G^* (b) and (d) measured in sample OG1 as a function of frequency at different temperatures.

surements of partially molten granite samples were carried out step-wise between 20 and 0.002 Hz with successive frequencies differing by a factor of 2. The raw data yield the absolute value of the complex shear modulus $G^*(\omega)$ and the phase shift $\varphi(\omega)$ between applied torque and resultant deformation at different temperatures where $\omega = 2\pi f$ and f is an oscillation frequency in Hz. The measured shear modulus and the phase shift are shown in Fig. 4 for sample OG1 and in Fig. 5 for sample QFP. Real (G') and imaginary (G'') components of shear modulus as well as real (η') and imaginary (η'') components of shear viscosity as a function of temperature can be calculated from:

$$G'(\omega) = G^*(\omega)\ \cos[\varphi(\omega)],$$

$$G''(\omega) = G^*(\omega)\ \sin[\varphi(\omega)] \quad (1a)$$

and

$$\eta'(\omega) = G''(\omega)/\omega,$$

$$\eta''(\omega) = G'(\omega)/\omega \quad (1b)$$

(e.g. Bagdassarov and Dingwell, 1993). With the frequency decrease, the absolute value of the complex shear modulus decreases and the phase shift between applied torque and resultant angular deformation increases up to $\pi/2$. The main drop of the shear modulus occurs over a limited frequency range. This interval of frequencies becomes narrower as the temperature increases (Fig. 4b, d and Fig. 5b, d).

The main difference in the phase shift behavior between the two samples is the frequency dependence at temperatures above 1120° (see Fig. 4a, c and Fig. 5a, c). At low temperatures in both samples there is an approximately linear dependence between $\log(\varphi)$ and $\log(\omega)$. At higher temperatures in sample OG1 this relationship is still valid but the slope becomes smaller. In sample QFP at temperatures above 1120°C the phase shift is constant (does not depend on frequency and temperature).

The data on the complex shear modulus permit the real component of shear viscosity to be calculated using Eq. 1b. The real component of shear viscosity in sample OG1 is frequency-independent at high temperatures indicating the existence of a Newtonian relaxed viscosity in this partially molten granite (Fig. 6a). For sample QFP this regime of rheological behavior is not attainable (Fig. 6b). The temperature (T)-dependence of the relaxed values of shear viscosity for OG1 is of the Arrhenian type with an activation energy of 385 ± 5 kJ/mol:

$$\log(\eta_{\text{relaxed}}) = -6.609 + \frac{20119}{T} \quad (2)$$

Results of the dilatometric measurements of shear viscosity also reveal strain-rate-independent rheological behavior of this sample up to a viscosity 10^{11} Pa s and strain-rate up to 10^{-5} s^{-1} (see Fig. 6c). Thus, the torsion experiments on sample OG1 with a strain rate of 0.5×10^{-1} s^{-1} to 5×10^{-1} s^{-1} and the parallel plate viscometry with a strain rate between 1×10^{-5} and 1×10^{-7} s^{-1} produce the same result for the shear viscosity of partially molten granite with about 40 vol% of crystals. For composite viscoelastic materials the activation energy of viscous flow coincides with the activation energy of viscous flow of the continuous phase, i.e. with the activation energy of melt viscosity (Gittus, 1975).

For sample QFP the relaxed shear viscosity is unattainable in torsion experiments (Fig. 6b). The parallel-plate viscometry of the sample indicated a significant strain-rate dependence of shear viscosity of the sample. The data of unrelaxed shear viscosity obtained in a dilatometer with a strain-rate 10^{-5} s^{-1} plotted for comparison with sample OG1 (Fig. 6c). Unrelaxed viscosity data from torsion measured at 0.5×10^{-1} s^{-1} are close to the dilatometric measurements. It should be clear at this point that the measured shear viscosity in the sample with 55–60 vol% of crystals can be used for viscous flow modeling only in the case of small strain because it is sensitive to the microgeometry of the viscous phase which may change with time during the deformation of two phase composites (e.g. Bons, 1993; Bons and Urai, 1994). The activation energy of the viscous flow of sample QFP with a strain rate of 10^{-5} s^{-1} is 253 ± 12 kJ/mol and the Arrhenius equation for the unrelaxed shear viscosity is:

$$\log(\eta_{\text{unrelaxed}}) = -1.2557 + \frac{13237}{T} \quad (3)$$

The viscosity data measured in torsion deformation at low strain-rates ($<10^{-2}$ s^{-1}) or in parallel-plate viscometry ($<10^{-5}$ s^{-1}) are higher than the other values indicated in Fig. 6c and have larger activation energies (Table 2). From Fig. 6c it is evident that the unrelaxed shear viscosity of sample QFP at

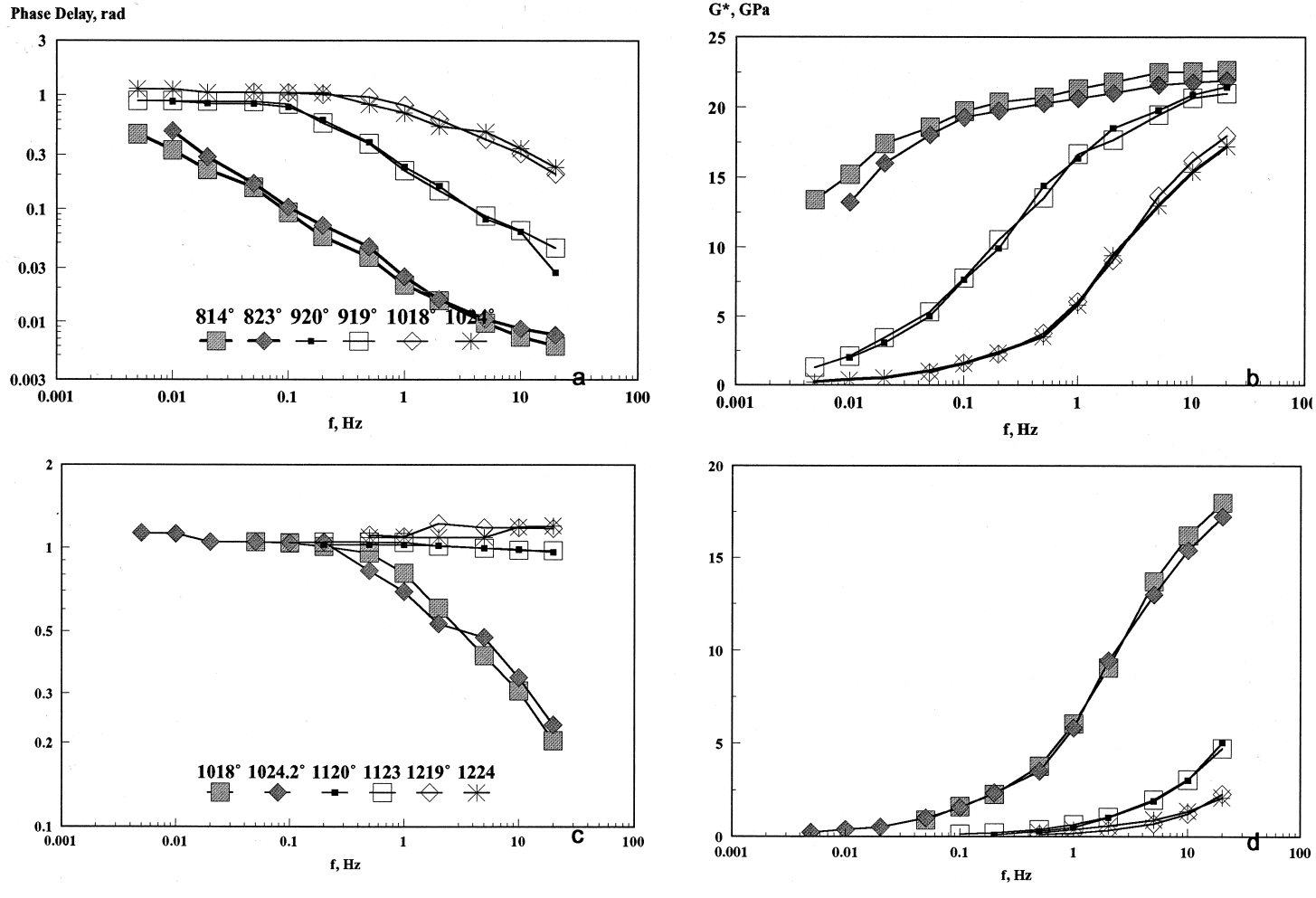

Fig. 5. Phase shift φ (a, c) and shear modulus G^* (b, d) measured in sample QFP as a function of frequency at different temperatures.

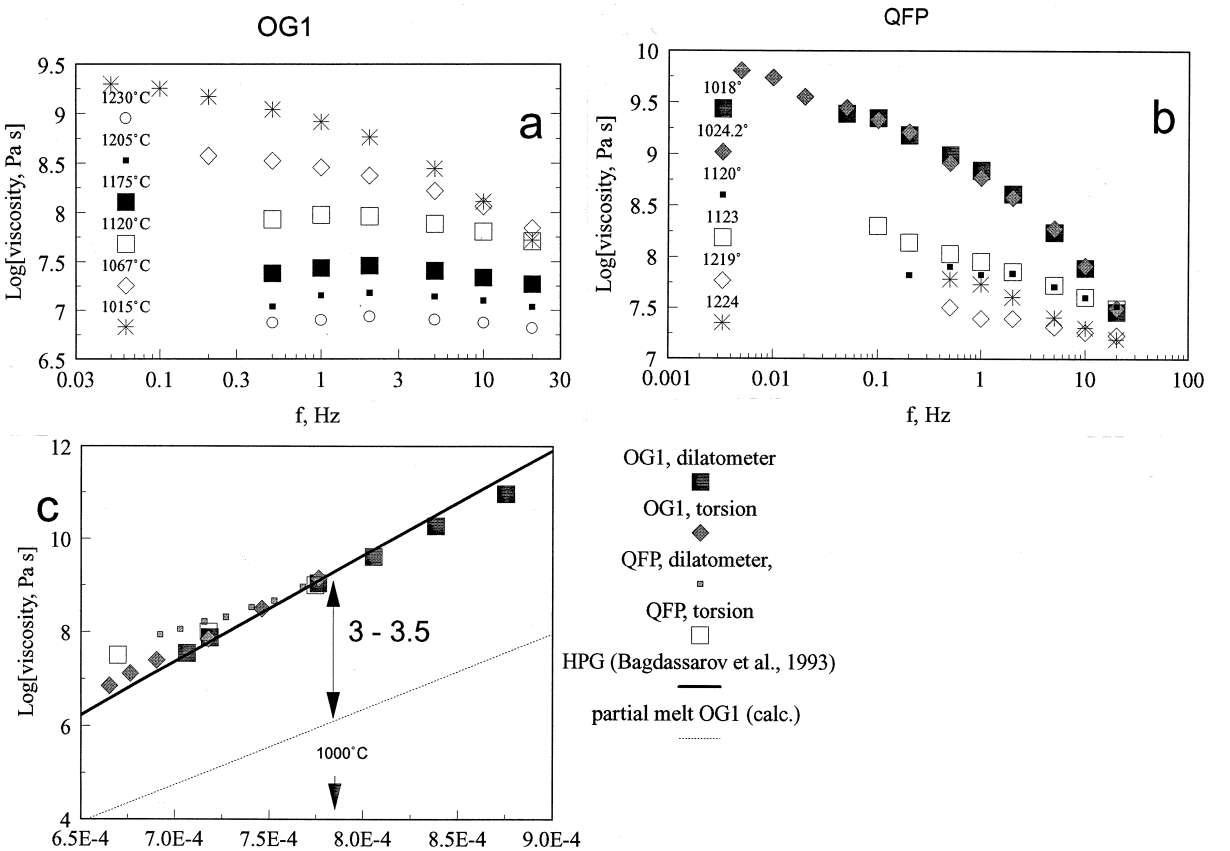

Fig. 6. Viscosity measured on partially molten granite samples QFP (a) and OG1 (b) with a simple shear method in a torsion oscillatory device as a function of frequency. Viscosity of partially molten granites obtained in the torsion device is compared with the data measured by the compression method in the dilatometer (c). The shear viscosity of the haplogranite melt (Bagdassarov et al., 1994) coincides with the viscosity of partially melted granites. At 1000°C the shear viscosity of the partial melt OG1 calculated from the Shaw (1972) method is 3–3.5 logarithmic units smaller.

low temperatures becomes even smaller than the relaxed shear viscosity of sample OG1 which contains fewer crystals. This paradox is due to the absence of a Newtonian viscosity in sample QFP.

Since the rheology of the partially molten granite sample OG1 is determined by the continuous melt phase, the viscoelastic behavior of the composite mimics the viscoelasticity of the partial melt. The difference in the absolute value of shear viscosity between partially molten sample OG1 and the pure melt of the same chemical bulk composition (HPG) is negligible (Fig. 6c). The difference in the absolute value of the shear viscosity between partially molten granites with 40 vol% of crystals and the calculated shear viscosity for the liquid phase alone of the partial melt composition (Table 1) using the Shaw method (1972) is 3–3.5 log(Pa s) units (Fig. 6c).

In contrast to sample OG1 there is no Newtonian rheology in sample QFP (Fig. 6b). The viscosity of sample QFP is strain-rate-dependent. In torsion experiments this strain-rate-dependence is due to weak mechanical interaction of crystals. The high concentration of crystals results in a non-zero shear modulus for the aggregate even at low frequencies and high temperatures. In long-duration dilatometric runs the shear viscosity is also unattainable because of the continuously changing microgeometry of the viscous phase. Experimentally measured shear viscosities of samples OG1 and QFP from dilatometric and torsional experiments are listed in Table 2.

Table 2
Viscosity of partially molten granite samples

T (°C)	$\log(\eta)$ (Pa s)	$\pm \log(\Delta\eta)$ (Pa s)	Strain rate (s^{-1})
Sample OG1			
Dilatometer			
869.3	10.97	0.16	1.0×10^{-7}
919.7	10.27	0.14	2.9×10^{-7}
967.9	9.61	0.07	6.1×10^{-7}
1015.3	9.04	0.09	1.4×10^{-6}
1118.8	7.88	0.11	2.0×10^{-5}
1142.4	7.55	0.09	4.1×10^{-5}
Torsion			
1015	9.15	0.14	5.0×10^{-2}
1067	8.50	0.09	2.0×10^{-1}
1120	7.85	0.12	5.0×10^{-1}
1175	7.40	0.11	5.0×10^{-1}
1205	7.12	0.18	5.0×10^{-1}
1230	6.85	0.06	5.0×10^{-1}
Sample QFP			
Dilatometer			
1029.9	8.77 [a]	0.17	3.5×10^{-4}
1029.3	8.97 [a]	0.06	1.5×10^{-5}
1055.0	8.42 [a]	0.09	1.6×10^{-4}
1055.3	8.67 [a]	0.13	4.7×10^{-5}
1077.8	8.22 [a]	0.15	3.1×10^{-4}
1077.0	8.53 [a]	0.12	5.1×10^{-5}
1102.1	8.20 [a]	0.08	2.1×10^{-4}
1102.4	8.32 [a]	0.07	8.2×10^{-5}
1124.9	7.99 [a]	0.16	2.5×10^{-4}
1124.1	8.22 [a]	0.10	6.5×10^{-5}
1149.2	7.79 [a]	0.12	3.5×10^{-4}
1149.4	8.06 [a]	0.11	1.5×10^{-5}
1171.0	7.94 [a]	0.13	1.9×10^{-4}
Torsion			
1018	9.05[a]	0.18	5.0×10^{-1}
1120	8.03[a]	0.24	5.0×10^{-1}
1220	7.51[a]	0.11	5.0×10^{-1}

[a] Strain-rate dependent shear viscosity.

5. Complex shear modulus and internal friction Q^{-1}

The relaxed shear viscosity of sample OG1 may be calculated at a given temperature using Eq. 2. Data on relaxed shear viscosity for sample OG1 permit the shear stress relaxation time to be calculated using $\tau = \eta(0)/G(\infty)$, i.e. the ratio of relaxed shear viscosity to the unrelaxed shear modulus. The variable τ has the same temperature dependence or activation energy as the relaxed shear viscosity. Data on the shear modulus and phase shift measured at different frequencies and temperatures may be reduced to a master plot using normalized non-dimensional frequency $\omega\tau$ (e.g. Nowick and Berry, 1972). This procedure of data reducing for both temperature- and frequency-dependence through dimensionless variable $\omega\tau$ is essentially based on the assumption that there is a single temperature-dependent relaxation time $\tau(T)$ obeying an Arrhenius relationship for temperature. In the case of a set of relaxation times this strategy may be also applied, assuming that the entire distribution of relaxation times has a similar temperature dependence with close values of activation energies. Alternatively, a more sophisticated fit of a master plot may be done using a non-Arrhenian relationship, for example $\tau \propto \exp(E_a/RT)^n$ or a Vogel–Fulcher–Tamman equation. In this paper we used a simple Arrhenian temperature dependence for fitting the data.

For reducing data on the internal friction and the shear modulus of sample QFP on master plots we have used the activation energy of the peak of the imaginary component of the shear modulus $G^*(\omega)$. The logarithm of frequency corresponding to a maximum value of $G''(\omega)$ depends linearly on $1/T$ (K). The slope of the $\ln(\omega_{\text{peak}})$ vs. $1/T$ (K) trajectory has an activation energy of 440 kJ/mol which is significantly larger than the value obtained from the unrelaxed shear viscosity data.

Viscoelastic behavior of materials is also characterized by the internal friction or the loss tangent, i.e. the inverse of the mechanical quality factor:

$$Q^{-1}(\omega) = \frac{G''(\omega)}{G'(\omega)} = \tan[\varphi(\omega)] \tag{4}$$

For both samples internal friction was calculated using data from Figs. 4 and 5. The master plots of normalized real and imaginary components of the shear modulus and internal friction for sample OG1 are shown in Fig. 7a and Fig. 8a, for sample QFP in Fig. 7b and Fig. 8b. For sample OG1 the logarithm of internal friction is approximated by a straight-line dependency vs. $\log(\omega\tau)$ (see Fig. 8a). The experimental dependency is as follows:

$$Q^{-1}(\omega\tau) \propto \frac{1}{(\omega\tau)^{\alpha}} \tag{5}$$

where for sample OG1 $\alpha \approx 0.5$ according to our

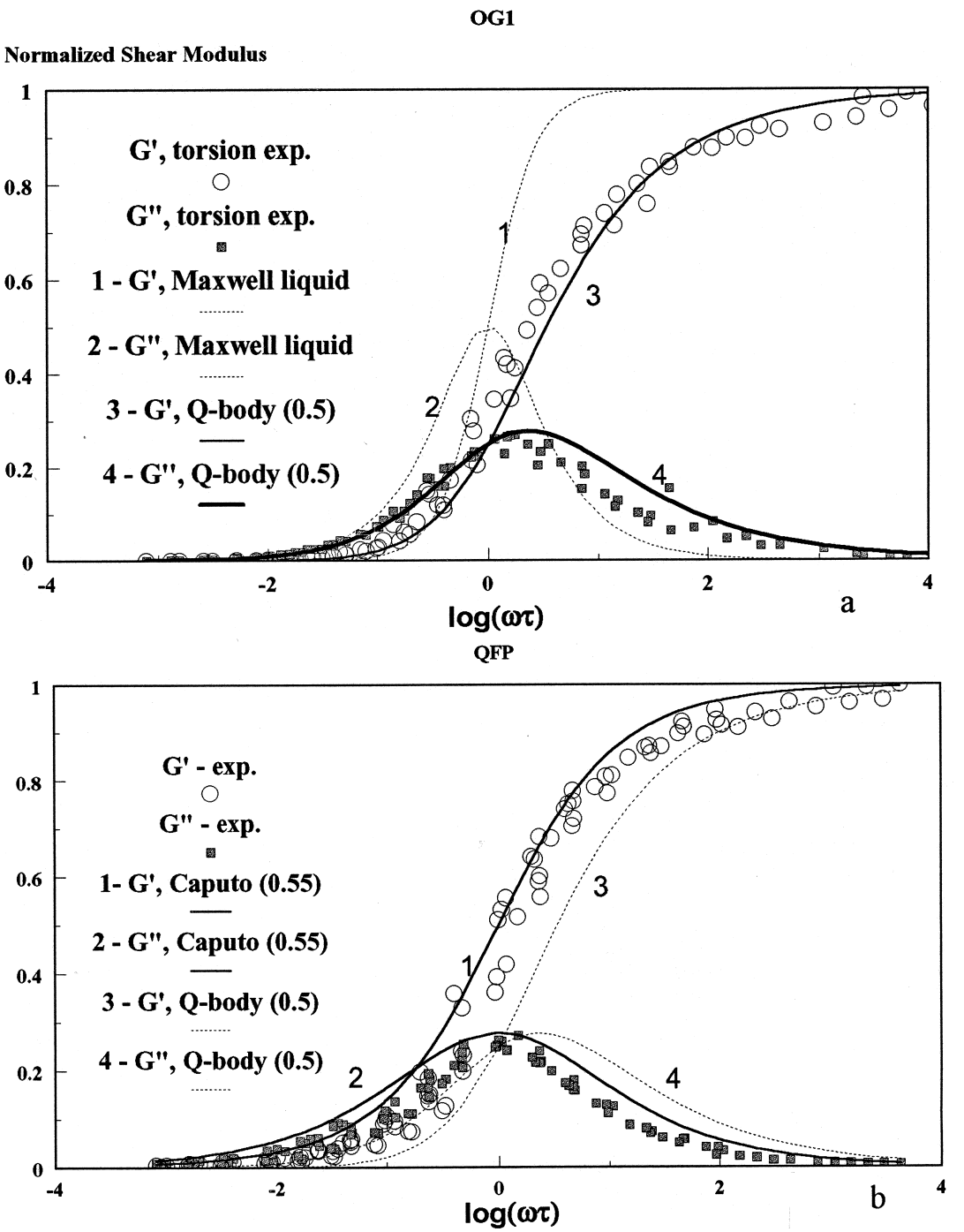

Fig. 7. Master curves of the normalized complex shear modulus (a) and internal friction (b) of sample OG1 as a function of $\log(\omega\tau)$. In (a) curves *1* and *2* are the calculated real and imaginary components of the normalized shear modulus of a Maxwell liquid; curves *3* and *4* are the calculated G' and G'' for a power law Q-body $Q^{-1} \propto (1)/((\omega\tau)^{0.5})$. In (b) curves *1* and *2* G' and G'' are calculated for a Caputo-body with the exponent 0.55.

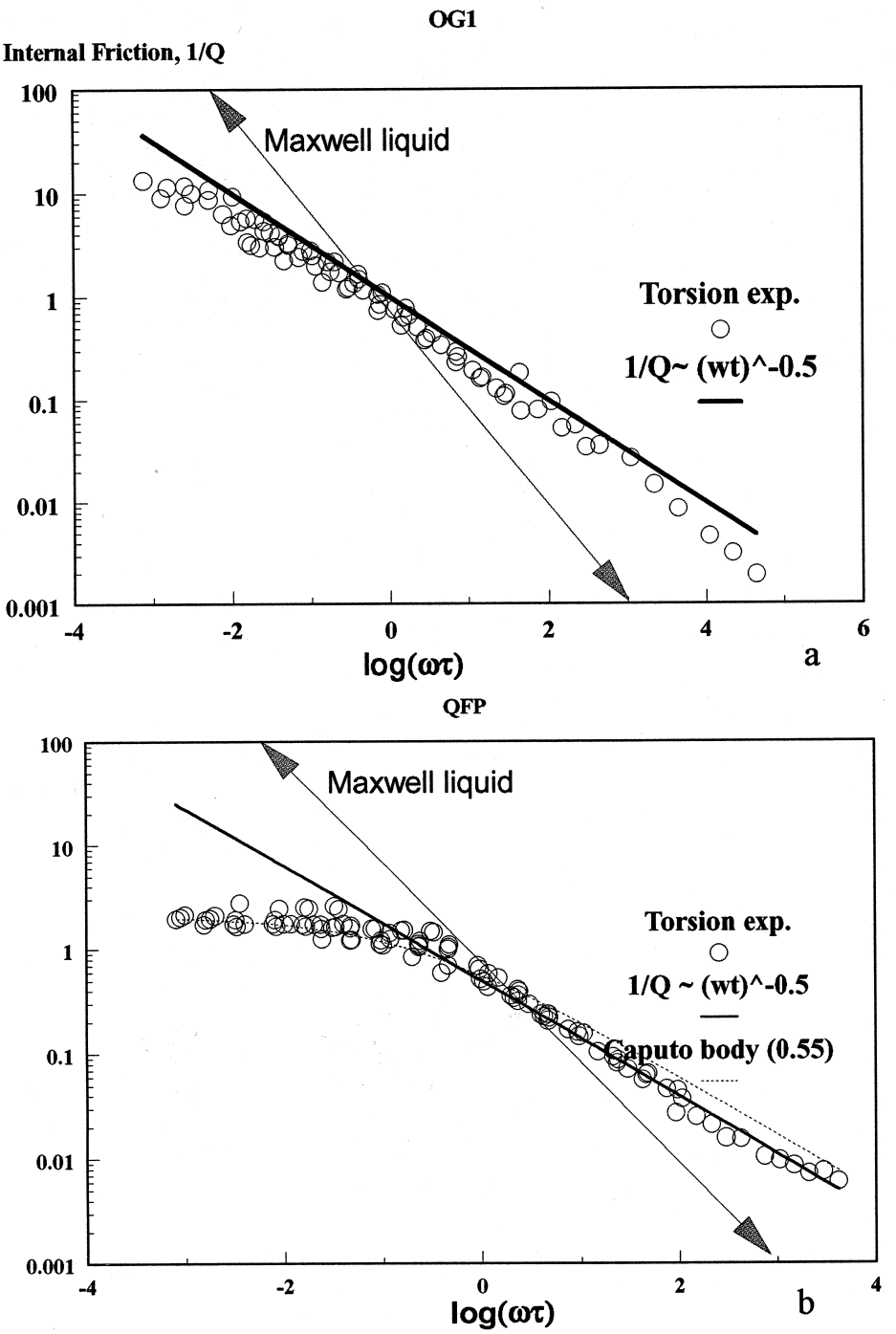

Fig. 8. Master curves of complex shear modulus (a) and internal friction (b) of QFP sample $\log(\omega\tau)$. In (a) the solid line is the calculated quality factor of a power law Q-body with the exponent 0.5. In (b) the solid line is the calculated quality factor of a power law Q-body with the exponent 0.5; the dashed line is the Caputo-body with the exponent 0.55.

experimental data. This type of relationship between internal friction and normalized frequency is known as a power law Q-body (e.g. Müller, 1983). Eq. 5 with an exponent of 0.5 is typical for the viscoelastic behavior of rhyolitic and granitic melts (Bagdassarov and Dingwell, 1993). On a double logarithmic plot the slope of $\log(Q^{-1})$ is -0.5 for $\omega\tau > 1$. In the range $\omega\tau < 1$ the slope becomes smaller (~ -0.45). The master plot for the real and imaginary components of the shear modulus of sample OG1 can also be approximated by a power law Q-body with $\alpha = 0.5$ (see Fig. 7a):

$$\frac{G(\omega\tau)}{G(\infty)} = \frac{(\omega\tau)^{1.5} + i\omega\tau}{1 + (\omega\tau)^{0.5} + \omega\tau + (\omega\tau)^{1.5}} \tag{6}$$

Eq. 6 can be derived from the theoretical viscoelastic modulus of power law Q material for the special case when the exponent in the power law is the reciprocal of a natural number 2, in this case (Müller, 1983).

The internal friction and complex shear modulus of sample QFP are shown in Fig. 7b and Fig. 8b. At $\omega\tau > 1$ the internal friction depends on $\omega\tau$ as $Q^{-1} \propto (\omega\tau)^{-0.5(\pm 0.05)}$. At $\omega\tau < 1$ the internal friction is practically constant $Q^{-1} \approx 2$. The shape of the imaginary component of the shear modulus is symmetrical with a maximum value of 0.25. Similar behavior of internal friction and the complex shear modulus has been observed in a suspension of spherical crystals in a rhyolite melt (Bagdassarov et al., 1994). Thus, in the case of sample QFP the anelastic behavior and the shear modulus can be ascribed to a Caputo-body model, i.e. an anelastic solid with an almost constant internal friction at $\omega\tau \ll 1$ (Caputo, 1967). In this case the frequency dependence of the internal friction and the complex shear modulus can be approximated as follows:

$$Q^{-1}(\omega\tau) = \frac{\sin\left(\frac{\gamma\pi}{2}\right)}{\cos\left(\frac{\gamma\pi}{2}\right) + (\omega\tau)^{\gamma}} \tag{7a}$$

and

$$\frac{G(\omega\tau)}{G(\infty)} = \frac{(i\omega\tau)^{\gamma}}{1 + (i\omega\tau)^{\gamma}} \tag{7b}$$

(Caputo, 1967). In both samples OG1 and QFP the internal friction of partially molten granites at $\omega\tau \gg 1$ is characterized by the power law of $Q \propto (\omega\tau)^{0.5}$.

The frequency dependence of the complex shear modulus and internal friction of partially molten granite samples in Fig. 7 evidently differs from those for a Maxwell liquid:

$$Q^{-1} = \frac{1}{\omega\tau} \tag{8a}$$

and

$$\frac{G(\omega\tau)}{G(\infty)} = \frac{i\omega\tau}{1 + i\omega\tau} \tag{8b}$$

A Maxwell liquid is an idealized viscoelastic model characterized by a single relaxation time $\tau = \eta(0)/G(\infty)$ (Nowick and Berry, 1972). If empirical parameters in Eq. 5 $\alpha = 1$ or in Eq. 7a and Eq. 7b $\gamma = 1$, these expressions become identical to those of a Maxwell liquid (Eq. 8a and Eq. 8b). A Caputo body is characterized by almost frequency-independent dissipation at low normalized frequencies $\omega\tau \ll 1$ which is the case for sample QFP (Fig. 8b). The observed peak of the imaginary component of the shear modulus for sample QFP is much wider than that of the Maxwell liquid model (Fig. 8a), with the extended shoulder in the range $\omega\tau > 1$. The maximum value of the imaginary component is 0.28 instead of 0.5 for the Maxwell liquid. These differences in the shape of the observed complex shear modulus and that for a Maxwell liquid indicate that the relaxation spectrum of partially molten granites is not a single relaxation time. It consists of a set of relaxation times in the range of several orders of magnitude. In general the observed master plots of the complex shear modulus of samples OG1 and QFP indicate the viscoelastic behavior with a wide spectrum of relaxation times extended to the range $\omega\tau \gg 1$ which is typical for silicate melts (Bagdassarov et al., 1994).

6. Discussion: viscoelastic model of partially molten granites

The data on the complex shear modulus and internal friction of two granite samples can be applied to the prediction of elastic wave dispersion and creep functions of partially molten granites. In laboratory experiments using ultrasonic frequencies only unrelaxed values of shear modulus can be measured. Correct interpretation of seismic data on dispersion and propagation of shear waves requires that these

data are extrapolated to seismic frequencies. Using the relationship between the shear wave velocity and the normalized frequency $V(\omega,\tau)$ or $V(\omega,T)$ the extrapolation of laboratory ultrasonic data $V(\infty)$ to the seismic range of frequencies is possible.

In the case of power-law dependence of the internal friction $Q \propto (\omega\tau)^{0.5}$ for the sample OG1 with 60 vol% of melt the complex shear wave velocity $V(\omega\tau)$ is:

$$V(\omega\tau) = V(\infty)\sqrt{\left[\frac{(\omega\tau)^{1.5} + i\omega\tau}{1 + (\omega\tau)^{0.5} + \omega\tau + (\omega\tau)^{1.5}}\right]} \quad (9)$$

where $V(\infty)$ is the unrelaxed value of shear wave velocity corresponding to the case of the unrelaxed shear modulus.

This expression for the high-frequency approximation $\omega\tau \gg 1$ gives the following results:

$$V(\omega\tau) \approx V(\infty)\sqrt{1 + \frac{i}{\sqrt{\omega\tau}}} \approx V(\infty)\left(1 + \frac{i}{2\sqrt{\omega\tau}}\right) \quad (10)$$

(Müller, 1983). The real part of Eq. 10 is the phase velocity, the imaginary part stands for the attenuation. In the low-frequency approximation $\omega\tau \ll 1$ the complex shear wave velocity for sample OG1 may be approximated by:

$$V(\omega\tau) \approx V(\infty)(1+i)\sqrt{\frac{\omega\tau}{2}} \quad (11)$$

It follows from Eq. 11 that the shear wave vanishes at low frequency–high temperatures, simply implying that at this range of $\omega\tau \ll 1$, stress and strain are shifted in phase with respect to each other by $\pi/2$.

For the partially molten sample QFP the high frequency approximation (Eq. 11) is also valid for $Q \gg 1$. In the low frequency–high temperature range the complex shear wave velocity depends on $\omega\tau$ as follows:

$$V(\omega\tau) = V(\omega_0\tau_0)\left(\frac{i\omega\tau}{\omega_0\tau_0}\right)^{\frac{2}{\pi}\arctan\left[\frac{1}{Q(\omega_0\tau_0)}\right]} \quad (12)$$

(Müller, 1983), where $\omega_0\tau_0 \approx 3$ is the onset of the constant internal friction behavior of sample QFP (see Fig. 8b). From experiments with partially molten sample QFP the exponent in Eq. 12 is about 0.7.

The stress-relaxation functions for the short-time approximation derived from the high-frequency Eq. 10 in both samples will behave similarly. From the theoretical analysis of the power law Q-body (Müller, 1983) we can predict that, if the partially molten granite was subjected to an instantaneous shear-stress step with an amplitude σ_o, the shear stresses would relax as follows:

$$\sigma(t) = \sigma_0 \exp\left(-\left[\frac{2t}{\tau}\right]^{0.5}\right) \quad (13)$$

where the exponent 0.5 is estimated from our experimental data. The relaxation function for the QFP sample at a low frequency–high temperature range decays as a power law, $\sigma(t) \propto t^{-0.7}$. Thus, the onset of the power law creep for the partially molten granite QFP is at $\omega\tau \approx 3$. For the sample OG1 the onset of the steady power law creep has not been observed up to $\omega\tau \sim 10^{-4}$.

For interpretation of seismic data it is important to know the temperature- and frequency-dependencies of shear wave velocity. From our experimental results $Q^{-1}(T)$ and $V(T)$ can be calculated for partially molten granite rocks using a Caputo-body viscoelastic model with a parameter 0.55 for a partially molten granite with 40 vol% of melt and a power law Q-body model for a granite containing 60 vol% of melt. Fig. 9 demonstrates the temperature dependence of internal friction (Fig. 9a) and complex shear wave velocity (Fig. 9b) at a frequency of 1 Hz. The temperature dependence of the relaxation time τ for sample OG1 is:

$$\log(\tau) = -17.079 + \frac{20119}{T} \quad (14a)$$

and for sample QFP:

$$\log(\tau) = -11.7257 + \frac{13237}{T} \quad (14b)$$

The arrows indicate the points where melting from 40 to 60 vol% occurred. When the melting fraction increases from 40 to 60 vol% an increase of Q^{-1} of about one order of magnitude is expected. The decrease in shear wave velocity may be less than a factor of 2.

Our rheological data have been obtained in experiments with a few percent of strain, which would

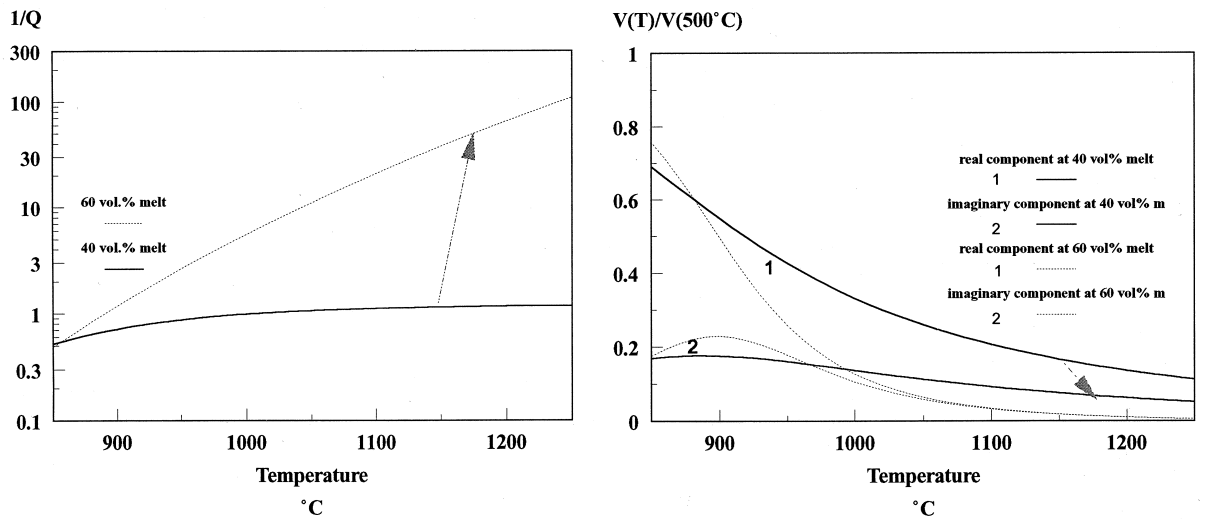

Fig. 9. Internal friction (a) and velocity of shear waves (b) as a function of temperature in partially molten granite samples. The arrows indicate the increase of the internal friction Q^{-1} and the drop of the shear wave velocity at 1 Hz, if the volume fraction of partial melt increases from 40 to 60 vol%.

make them relevant to processes of seismic wave propagation. In our situation of magma intruded into crustal rocks the strain is much larger. However, assuming that in a partially molten magma with 60–100 vol.% of melt the flow differentiation processes do not result in significant melt squeezing from the granite magma, we may be able to use the measured viscosity data to answer the question what is the shape of granite magma emplacement in crustal rocks. Viscoelastic behavior of partially molten granites will certainly influence the style of emplacement of granitic rocks into lithospheric host rocks. The difference in conditions between the emplacement of granitic dikes and diapirs has already been discussed in the literature assuming a Maxwell model of viscoelasticity for host rocks and Newtonian rheology for intruding magma (Rubin, 1993). Our results point to non-Newtonian and strain-rate-dependent rheology (Caputo-body model) for 'dry' partially molten granites with ≈40 vol% of melt, and power law Q-body for 'dry' granites containing ≈60 vol% of melt. In the latter case we still can consider partially molten granite as a Newtonian liquid.

The difference in Newtonian shear viscosity between 'dry' haplogranitic granitic melt (Bagdassarov et al., 1994) and 'dry' partially molten granite with 60 vol% of melt is negligible. The viscosity of quartzite rocks in the temperature interval 1100–1000ºC under 100 MPa of stress (Gleason and Tullis, 1995) exceeds the viscosity of partially molten granites (40–60 vol% of melt) by ≈4.1 to 4.0 log units. According to the analysis of Rubin (1993) the shape of intrusion of partially molten to pure molten granite magma (60–100 vol.% of melt fraction) into quartzite rocks will be close to the equidimensional shape, due to the moderate contrast between the magma viscosity and the host rocks ($\log[(\eta_{\text{magma}})/(\eta_{\text{hostrocks}})] \approx -4$) at the expected value of the elastic parameter ($(P_{\text{emplacement}})/(G_{\text{hostrocks}}) \approx 10^{-3}$ to 10^{-4}) (where $P_{\text{emplacement}}$ is the excess of pressure in the magma relative to the lithostatic pressure and $G_{\text{hostrocks}}$ is the elastic stiffness of the host rock). The frequently observed fracturing and dike propagation of granite magma in crustal rocks actually shows a much higher viscosity contrast between magma and host rock. This may occur when the intrusion of the granite occurs at temperatures above the solidus into cold host rocks. Then, with time, the shape of the initial granite intrusion may also evolve from a narrow dike into an equidimensional pluton, because partially molten granite may transport sufficient heat to reduce the effective viscosity of surrounding rocks. Due to the heat exchange with host rocks the degree of partial melting of the magma decreases and the effective viscosity increases, resulting in a smaller

viscosity contrast between magma and host rocks. If the size, temperature and rheology of the reheated aureole permit large-scale ductile strains in the volume surrounding the dike, the initially narrow dike widens and the tip of the dike may become significantly blunted with time.

7. Conclusions

(1) Two different viscoelastic behaviors have been observed in partially molten granite samples. In those where the crystal fraction is below the rheologically critical 40 vol% the overall behavior is characterized by the power law Q-body with the exponent 0.5–0.55. In those with a crystal content of >40 vol% the internal friction is characterized by a Caputo-body with the parameter 0.55 and non-zero shear modulus at $\omega\tau \ll 1$.

(2) The creep function short-time-scale deformation ($\omega\tau > 1$) in partially molten granites has a stretched exponential dependence on time with the parameter 0.5. If the percentage of melt phase is greater than 60 vol% this dependence is expected to be linearly proportional with time for long-time-scale deformation processes ($\omega\tau < 1$). If the percentage of melt is less than 40 vol% the creep function has a power law dependence with an exponent of ≈0.5.

(3) The viscosity contrast between melted and 40–60 vol% partially melted granites is negligible. The viscosity contrast between the melt corresponding to 60 vol% of granite melting and the effective viscosity of partially melted granite rock is about 3–3.5 log(Pa s) units. Effect of 40 vol% of crystals on granite melt viscosity may be partially compensated by the viscosity changes due to the chemical composition of partial granite melt (mainly due to variations in SiO_2 and alkalis).

Acknowledgements

This work has been done at the Bayerisches Geoinstitut, Universität Bayreuth. The postdoctoral support for the authors has been provided by D. Dingwell (BGI, Bayreuth). The authors are grateful to H. Schulze and G. Herrmannsdörfer for technical help and sample preparation, D. Krauße (all BGI, Bayreuth) for microprobe analysis, O. Eklund (ABO, Turku) and R. Thomas (GFZ, Potsdam) for samples of granites, Y. Bottinga (IPGT, Paris) and H. Pinkerton (ES, Lancaster), E. Rutter (University Manchester) and an anonymous reviewer for their constructive comments on the manuscript.

References

Andersson, U.B., Eklund, O., 1994. Cellular plagioclase intergrowths as a result of crystal-magma mixing in the Proterozoic Åland rapakivi batholith, SW Finland. Contrib. Mineral. Petrol. 117, 124–136.

Bagdassarov, N., Dingwell, D., 1992. A rheological investigation of vesicular rhyolite. J. Volcanol. Geotherm. Res. 50, 307–322.

Bagdassarov, N., Dingwell, D., 1993. Frequency dependent rheology of vesicular rhyolite. J. Geophys. Res. 98, 6477–6487.

Bagdassarov, N.S., Dingwell, D.B., Webb, S.L., 1994. Effect of boron, phosphorus, and fluorine on shear relaxation in haplogranite melts. Eur. J. Mineral. 5, 409–425.

Berckhemer, H., Kampfmann, W., Aulbach, E., 1982. Anelasticity of mantle rocks near partial melting. In: Schreyer, W. (Ed.), High Pressure Research in Geosciences. Schweizerbart, Stuttgart, pp. 113–132.

Bons, P.D., 1993. Experimental Deformation of Polyphase Rock Analogues. PhD Thesis No 110, Faculty of Geosciences, University Utrecht, 207 pp.

Bons, P.D., Urai, J.L., 1994. Experimental deformation of two-phase rock analogues. Mat. Sci. Eng. A 175, 221–229.

Caputo, M., 1967. Linear models of dissipation whose Q is almost frequency independent, II. Geophys. J.R. Astron. Soc. 13, 529–539.

Gerstenberger, H., Haase, G., Wemmer, K., 1995. Isotope systematic of the Variscan postkinematic granites in the Erzgebirge (E-Germany). Terra Nostra 7, 36–41.

Gittus, J., 1975. Creep, Viscoelasticity, and Creep Fracture in Solids. Applied Science Publishers, London, pp. 426–431.

Gleason, G.C., Tullis, J., 1995. A flow law for dislocation creep of quartz aggregates determined with the molten salt cell. Tectonophysics 247, 1–23.

Jackson, I., 1986. The laboratory study of seismic wave attenuation. In: Hobb, B.E., Heard, H.C. (Eds.), Mineral and Rock Deformation, Laboratory Studies — The Paterson Volume. Am. Geophys. Union, Geophys. Monogr. 36, 11–23.

Jackson, I., Paterson, M.S., 1987. Shear modulus and internal friction of calcite rocks at seismic frequencies: pressure, frequency and grain size dependence. Phys. Earth Planet. Inter. 45, 349–367.

Jackson, I., Paterson, M.S., Fitz-Gerald, J.D., 1992. Seismic wave dispersion and attenuation in Åhem dunite: an experimental study. Geophys. J. Int. 108, 517–534.

Kampfmann, W., 1984. Laborexperimente zum elastischen und anelastischen Verhalten hochtemperierter magmatischer Gesteine im Frequenzbereich seismischer Wellen. Dissertation im Fachbereich Geowissenschaften, J.W. Goethe Universität zu Frankfurt am Main, 137 pp.

Leong, E.C., Randolph, M.F., 1992. A model for rock interfacial behavior. Rock Mech. Eng. 25 (3), 187–206.

Lindberg, B., Eklund, O., 1992. Mixing between basaltic and granitic magmas in a rapakivi related quartz-feldspar porphyry, Åland, SW Finland. Geol. Fören. Stockholm Förh. 14, 103–112.

Müller, G., 1983. Rheological properties and velocity dispersion of a medium with power-law dependence of *Q* on frequency. J. Geophys. 54, 20–29.

Nowick, A.S., Berry, B.S., 1972. Anelastic Relaxation in Crystalline Solids. Academic Press, San Diego, Calif., 678 pp.

Rubin, A., 1993. Dikes vs. diapirs in viscoelastic rocks. Earth Planet. Sci. Lett. 117, 653–670.

Shaw, H.R., 1972. Viscosities of magmatic silicate liquids. Am. J. Sci. 252, 870–893.

Smith, B.K., Carpenter, F.O., 1987. Transient creep in orthosilicates. Phys. Earth Planet. Inter. 49, 314–324.

Tischendorf, G., 1989. Silicic magmatism and metallogenesis of the Erzgebirge. ZIPE, Potsdam, pp. 52–60.

Tischendorf, G., Geisler, M., Gerstenberger, H., Budzinski, H., Vogler, P., 1987. Geochemistry of Variscan granites of the Westerzgebirge–Vogtland region — an example of tin deposit-generating granites. Chem. Erde 46, 213–235.

Tsenn, M.C., Carter, N.L., 1987. Upper limits of power-law creep of rocks. Tectonophysics 136, 1–26.